



9th International Conference on Applied Energy, ICAE2017, 21-24 August 2017, Cardiff, UK

## Comparison of numerical efficiency of the thermal and the kinetic rate drying model applied to a thermally thick wood particle

Inge Haberle<sup>a,\*</sup>, Nils Erland L. Haugen<sup>a,b</sup>, Øyvind Skreiberg<sup>b</sup>

<sup>a</sup>Department of Energy and Process Engineering, Norwegian University of Science and Technology, NTNU, Kolbjørn Hejes vei 1B, 7491 Trondheim, Norway

<sup>b</sup>Department of Thermal Energy, SINTEF Energy Research, Postboks 4761 Torgard, 7465 Trondheim, Norway

---

### Abstract

In this work, the drying and devolatilization of a thermally thick wood particle were modeled. The work was validated against experiments and good agreement was found. The work compared the numerical efficiency and accuracy of the thermal drying model and the kinetic rate drying model. The thermal drying model was used with a fixed boiling temperature (373 K). The kinetic data for the kinetic rate drying model was taken from an earlier work by Di Blasi [1] and additionally one set of kinetic data that was also tested, was assumed by the authors, with the main purpose of reducing the stiffness of the evaporation equation. The numerical efficiency was compared by comparing the CPU times associated with the different drying models. It was found that the thermal drying model is the most efficient drying model at both high and low moisture contents. Soft drying kinetics resulted in intermediate CPU times, while very stiff kinetics yielded the lowest numerical efficiency. No trend was observed regarding how CPU times of the different drying models behave with respect to increasing or decreasing moisture contents.

© 2017 The Authors. Published by Elsevier Ltd.

Peer-review under responsibility of the scientific committee of the 9th International Conference on Applied Energy.

*Keywords:* drying, devolatilization, mesh-based model, one-dimensional, accuracy, numerical efficiency, thermally thick, wood

---

### 1. Introduction

Due to its superiority with respect to CO<sub>2</sub> emissions, emitting zero net CO<sub>2</sub>, biomass is often preferred over fossil fuels [2]. Therefore, research within the field of modeling of thermochemical degradation of biomass has been

---

\* Corresponding author. Tel.: +47 73 593697.

E-mail address: [inge.haberle@ntnu.no](mailto:inge.haberle@ntnu.no)

intensified over the last years. By obtaining a deeper understanding of drying, devolatilization as well as char conversion of biomass, one can optimize current combustion units, with the objective of operating those units at even lower emissions. This is not only strengthening the advantages of biomass over fossil fuels but is also inevitably required since emission limits for biomass combustion units become stricter [3]. A numerically efficient simulation tool is crucial when it comes to using numerical simulations for design and development of new combustion units. Those tools will be of significant importance in the future, since they are cheap and less time-consuming compared to experimental tests [4], which makes them the preferential optimization and design route of furnace manufacturers. It may be surprising that, despite its physically simple nature, drying is found to be a computationally intensive stage of the thermal conversion. A computationally fast model for drying is therefore a chief feature of an efficient thermal conversion model.

In this work, a one-dimensional simulation tool for drying and devolatilization of thermally thick cylindrical wet wood particles was developed, with the main purpose of obtaining a deeper understanding on how these two stages can be accurately modeled in a numerically efficient manner. The model was mesh-based and validated against experiments by Lu et al. [5]. Different drying models were investigated with the main purpose of discussing numerical efficiency and model accuracy. In this work, the thermal drying model and the kinetic rate drying model were compared. The authors also aimed to identify a set of kinetic drying data for the kinetic rate model that was supposed to reduce the stiffness of the evaporation reaction, while meanwhile yielding acceptable accuracy and improved numerical efficiency.

## 2. Model

The IDA solver included in SUNDIALS (SUite of Nonlinear and Differential/ALgebraic Equation Solvers) [6] was used to solve the governing equations in a fully implicit manner. More details on the governing equations can be found elsewhere [5]. The only main differences between the model by Lu et al. [5] and the model used in the current paper were that re-condensation of liquid free water was neglected in the current work and furthermore, that liquid free water movement in the current work was described by convection with the velocity derived from Darcy's law, as suggested by Grønli [7], with the permeability being  $\kappa_l = 10^{-20} \text{ m}^2$ . Shrinkage was modeled with the three-parameter model of Di Blasi [8] with the shrinkage parameters being  $\alpha = 1, \beta = 0.75, \gamma = 1$ . The integration method was the backward-differentiation formula, with the order varying between 1 and 5. This integration method was a suitable choice as it can solve very stiff equations [6]. The number of grid points in the 1D mesh was chosen such that the modeling results were grid-independent. The tolerance of the solver was set to  $1 \times 10^{-3}$ .

The kinetic rate drying model describes evaporation with an Arrhenius expression [9]. The kinetic rate drying model in this model was always coupled to modeling liquid water transportation by diffusion, which equals a bound water assumption. The thermal drying model assumes drying to occur at a fixed boiling temperature, most commonly 373 K, and no further temperature increase is allowed before the entire moisture content of a cell volume has been evaporated. This results in a step-function which is known to cause numerical instabilities [9]. The thermal drying model in this model was always coupled to modeling liquid water transportation by convection, which equals a liquid free water assumption.

The main input data used in the simulations are listed in Table 1, where  $c_p$  is the specific heat capacity,  $\Delta h_{evap}$  is the latent heat of evaporation,  $\Delta h_{devol,1}$  is the heat of reaction of primary devolatilization,  $\Delta h_{devol,2}$  is the heat of reaction of secondary reactions,  $D$  is the effective diffusion coefficient of the gases,  $D_b$  is the diffusion coefficient of the bound water and  $\lambda$  is the thermal conductivity. The permeability of the solid phase is  $\kappa_{solid}$ . Subscripts  $w$ ,  $c$  and  $g$  refer to wood, char and gas phase, respectively.

Table 1. List of applied properties and the assigned values.

Property	Unit	Value	Reference
$c_{p,w}$	J/(kgK)	$1500 + T$	[9]
$c_{p,c}$	J/(kgK)	$420 + 2.09T + 6.85 \times 10^{-4} T^2$	[9]

$c_{p,g}$	J/(kgK)	1100	[8]
$\Delta h_{\text{evap}}$	kJ/kg	$-2.44 \times 10^3$	[5]
$\Delta h_{\text{devol},1}$	kJ/kg	-207	[10]
$\Delta h_{\text{devol},2}$	kJ/kg	42	[11]
D	m <sup>2</sup> /s	1E-6	[8]
$D_b$	m <sup>2</sup> /s	$7 \times 10^{-6} \exp((-4633 + 3523 M_b)/T)$	[7]
$\lambda_c (\parallel) / \lambda_c (\perp)$	W/(mK)	0.071 / 0.071	[5]
$\lambda_g$	W/(mK)	0.02577	[8]
$\lambda_w (\parallel) / \lambda_w (\perp)$	W/(mK)	$0.291 + 2.7588 \times 10^{-4} T / (\lambda_{\parallel} / 1.9)$	[12]
bridge factor, $\xi$	-	0.68	[13]
porosity, $\varepsilon$	-	0.62	
particle diameter	mm	9.5	[5]
aspect ratio	-	4	[5]
wood density	kg/m <sup>3</sup>	570 (poplar wood)	
$\kappa_{\text{solid}}$	m <sup>2</sup>	$1 \times 10^{-16}$	[14]

The boundary conditions of the temperature equation were modeled as suggested by Fatehi and Bai [15]. The pressure at the particle surface was set to ambient pressure. The species mass fraction boundary condition was a zero-gradient condition. In future work this boundary condition should be adjusted such that it accounts for the blowing effect of leaving volatiles. This blowing effect will also reduce the heat transfer coefficient. Devolatilization was modeled with the three independent competitive reactions scheme coupled with secondary tar reactions. The applied kinetics for drying and devolatilization are listed Table 2. Kinetic data of the soft-kinetics drying model were assumed by the authors in this work, without having been tested in earlier works. The assumption was based on kinetics originally suggested by Chan et al. [16] that were adjusted such that evaporation occurred within a temperature range of 373 to 473 K, which was considered acceptable as bound water evaporates at higher temperatures than 373 K. The same devolatilization kinetics as applied in the model by Lu et al. [5] were used in this model.

Table 2. Kinetic data used for drying and devolatilization.

Reaction	Pre-exponential factor A [1/s]	Activation energy $E_a$ [kJ/mol]	References
Drying, stiff-kinetics	$5.6 \times 10^8$	88	[1]
Drying, soft-kinetics	$5.13 \times 10^6$	55	assumed by the authors
Wood $\rightarrow$ Tar	$9.28 \times 10^9$	149	[5]
Wood $\rightarrow$ Char	$3.05 \times 10^7$	125	[5]
Wood $\rightarrow$ Permanent gases	$1.11 \times 10^{11}$	177	[5]
Tar $\rightarrow$ Permanent gases	$4.28 \times 10^6$	107.5	[5]
Tar $\rightarrow$ Char	$1 \times 10^5$	107.5	[5]

### 3. Results and Discussion

The model was validated against experimental results by Lu et al. [5] and the thermal drying model was used as a base case for comparisons regarding numerical efficiency. Good agreement was found, as can be seen in Fig. 1.

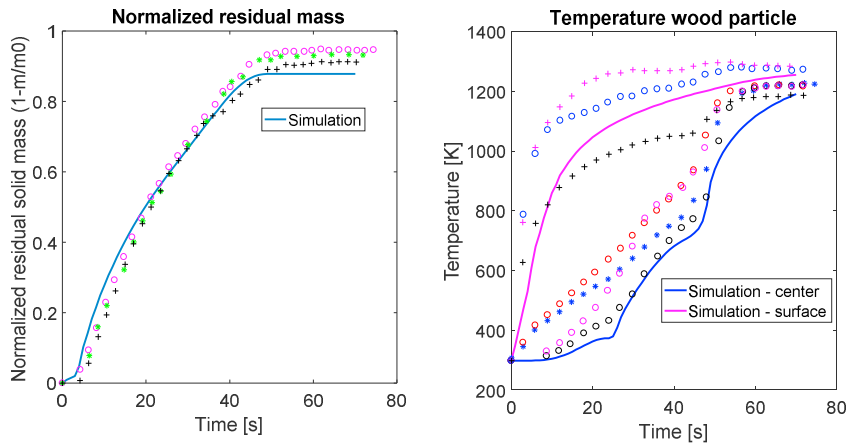


Fig. 1. Experimental data ( $\circ, *, +$ : mass;  $+, \circ, +$ :  $T_{\text{surface}}$ ;  $\circ, *, \circ, \circ$ :  $T_{\text{center}}$ ) [5] and model predictions (thermal drying model, 6 wt% w.b.).

Fig. 1 shows that the predicted mass of the wood particle initially decreases slightly faster in the numerical simulations compared to the experiments. The surface temperature agrees well with experimental findings. Since it is a valid assumption that the thermocouples were not exactly at the surface in the experiments, the surface temperature predicted in Fig.1 has not been taken exactly at the surface but a few grid points inwards.

Fig. 1 suggests that the assumption of a fixed boiling temperature is rather accurate, despite the fact that theoretically one expects an increase in boiling temperature due to increasing internal pressure caused by formation of water vapor. Still, a physically correct model should account for the influence of this pressure change. Furthermore, in Fig. 1 one can clearly see the temperature plateau at 373 K, where evaporation occurs. This plateau is even more prominent for higher moisture content, as seen in Fig. 2.

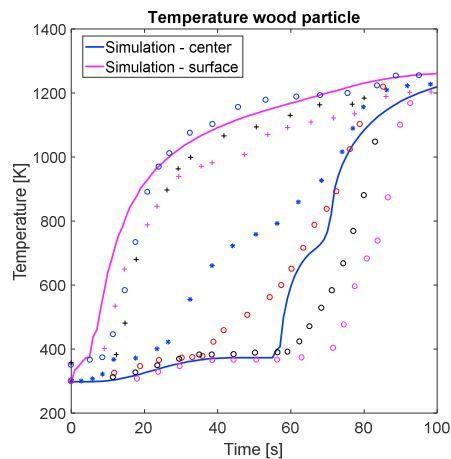


Fig. 2. Comparison experimental data ( $+, \circ, +$ :  $T_{\text{surface}}$ ;  $\circ, *, \circ, \circ$ :  $T_{\text{center}}$ ) [5] and model predictions (thermal drying model, 40 wt% w.b.).

After having validated the model and tested the thermal drying model, the kinetic rate drying model was tested and good agreement with experiments was found when using the kinetic rate drying model (Fig. 3 and Fig. 4). One can observe that the temperature plateau seen in Fig. 1 cannot be observed when applying the kinetic rate drying model (Fig. 3 and Fig. 4). For the stiff-kinetics drying model, the predicted center temperature of the wood particle showed the overall best agreement with the experimental results. The soft-kinetics drying model predicted a center temperature that deviated slightly more from the experiments than the stiff-kinetics drying model.

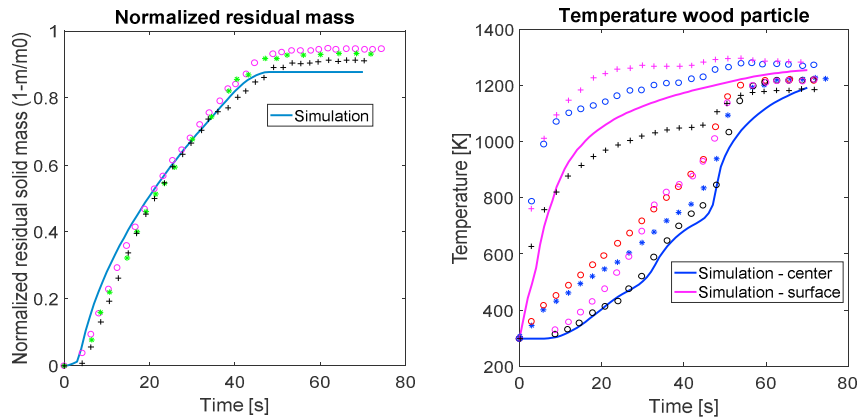


Fig. 3. Experimental data ( $\circ, *, +$ : mass;  $+, \circ, +$ :  $T_{\text{surface}}$ ;  $\circ, *, \circ, \circ$ :  $T_{\text{center}}$ ) [5] and model predictions (stiff-kinetics model, 6 wt% w.b.).

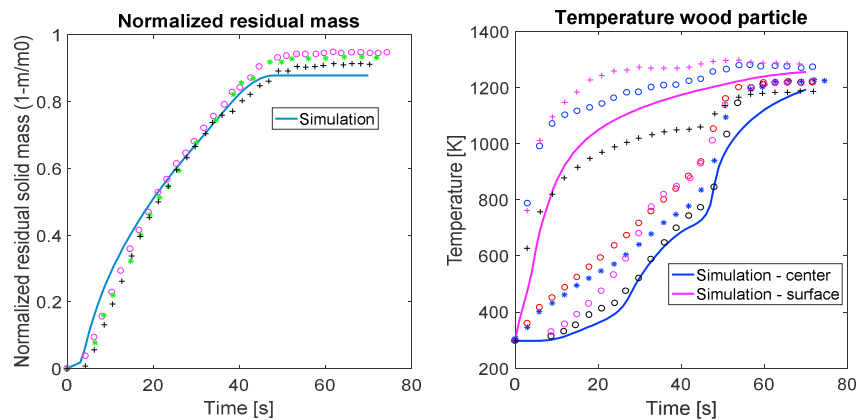


Fig. 4. Experimental data ( $\circ, *, +$ : mass;  $+, \circ, +$ :  $T_{\text{surface}}$ ;  $\circ, *, \circ, \circ$ :  $T_{\text{center}}$ ) [5] and model predictions (soft-kinetics model, 6 wt% w.b.).

The CPU times (Table 3) of the coupled drying and devolatilization model, when applying different drying models, were compared and it was found that the thermal drying model led to the most efficient drying simulations.

Table 3. Comparison of CPU times of different drying models.

Drying models	Final time [s]	Grid points	CPU time [s]
Drying, stiff-kinetics, 6 wt% (w.b.)	70	55	1085
Drying, soft-kinetics, 6 wt% (w.b.)	70	55	271
Thermal drying model, 6 wt% (w.b.)	70	55	278
Drying, stiff-kinetics, 40 wt% (w.b.)	100	55	710
Drying, soft-kinetics, 40 wt% (w.b.)	100	55	695
Thermal drying model, 40 wt% (w.b.)	100	55	463

Regarding numerical efficiency, the following observations with respect to the base case were made:

- At high moisture contents the soft-kinetics drying model is 1.5 times slower than the thermal drying model while the stiff-kinetics drying model is 1.53 times slower, and is therefore the slowest drying model.
- At low moisture contents the soft-kinetics drying model is approximately as fast as the thermal drying model, while the stiff-kinetics drying model is 3.9 times slower, and is therefore the slowest drying model.

#### 4. Conclusions and recommendations

Both drying models yield good agreement with experiments. It can be concluded that the kinetic rate drying model and the thermal drying model are reasonably accurate. It was found in the current model that the thermal drying model seems to be more numerically efficient. The optimized kinetic rate drying model (soft-kinetics) resulted in comparable CPU times for low moisture content test cases, while it was slower at higher moisture contents. The very stiff kinetic rate drying model (stiff-kinetics) seems to be the slowest drying model. The stiff-kinetics drying model resulted in the lowest efficiency for both high and low moisture contents. For low moisture contents it also resulted in significantly longer CPU times compared to the high moisture content drying. Therefore, one cannot identify a clear trend regarding how CPU times depend on the moisture content. It is therefore of interest to investigate this further in order to identify why longer convergence times are required when low moisture contents are modeled.

#### Acknowledgements

This work was carried out within the WoodCFD (243752/E20) project, which is funded by: Dovre AS, Norsk Kleber AS, Jøtulgruppen and Morsø AS together with the Research Council of Norway through the ENERGIX program.

#### References

- [1] Di Blasi C, Branca C, Sparano S, La Mantia B. Drying characteristics of wood cylinders for conditions pertinent to fixed-bed countercurrent gasification. *Biomass and Bioenergy* 2003;25:45–58.
- [2] Basu P. Chapter 1 - Introduction. In: Basu P, editor. *Biomass Gasification, Pyrolysis and Torrefaction*. Second, Boston: Academic Press; 2013, p. 1–27.
- [3] Scharler R, Benesch C, Neubeck A, Obernberger I. CFD Based Design and Optimisation of Wood Log Fired Stoves. Proc. 17th Eur. Biomass Conf. Exhib., Hamburg; 2009, p. 1361–7.
- [4] Skreiberg Ø, Seljeskog M, Georges L. The Process of Batch Combustion of Logs in Wood Stoves – Transient Modelling for Generation of Input to CFD Modelling of Stoves and Thermal Comfort Simulations. *Chem Eng Trans* 2015;43:433–8.
- [5] Lu H, Robert W, Peirce G, Ripa B, Baxter LL. Comprehensive Study of Biomass Particle Combustion. *Energy & Fuels* 2008;22:2826–39.
- [6] National Laboratory Lawrence Livermore. SUNDIALS: SUite of Nonlinear and Differential/ALgebraic Equation Solvers - IDA 2016. <http://computation.llnl.gov/projects/sundials/ida> (accessed April 7, 2017).
- [7] Grønli MG. A theoretical and experimental study of thermal degradation of biomass. The Norwegian University of Science and Technology, 1996.
- [8] Di Blasi C. Heat, momentum and mass transport through a shrinking biomass particle exposed to thermal radiation. *Chem Eng Sci* 1996;51:1121–32.
- [9] Mehrabian R, Zahirovic S, Scharler R, Obernberger I, Kleditzsch S, Wirtz S, et al. A CFD model for thermal conversion of thermally thick biomass particles. *Fuel Process Technol* 2012;95:96–108.
- [10] van de Velden M, Baeyens J, Brems A, Janssens B, Dewil R. Fundamentals, kinetics and endothermicity of the biomass pyrolysis reaction. *Renew Energy* 2010;35:232–42.
- [11] Koufopoulos CA, Papayannakos N, Maschio G, Lucchesi A. Modelling of the pyrolysis of biomass particles. Studies on kinetics, thermal and heat transfer effects. *Can J Chem Eng* 1991;69:907–15.
- [12] Pozzobon V, Salvador S, Bézian JJ, El-Hafi M, Le Maout Y, Flamant G. Radiative pyrolysis of wet wood under intermediate heat flux: Experiments and modelling. *Fuel Process Technol* 2014;128:319–30.
- [13] Biswas AK, Umeki K. Simplification of devolatilization models for thermally-thick particles: Differences between wood logs and pellets. *Chem Eng J* 2015;274:181–91.
- [14] Larfeldt J, Leckner B, Melaaen MC. Modelling and measurements of the pyrolysis of large wood particles. *Fuel* 2000;79:1637–43.
- [15] Fatehi H, Bai XS. A Comprehensive Mathematical Model for Biomass Combustion. *Combust Sci Technol* 2014;186:574–93.
- [16] Chan W-CR, Kelbon M, Krieger BB. Modelling and experimental verification of physical and chemical processes during pyrolysis of a large biomass particle. *Fuel* 1985;64:1505–13.